



# COORDINATED TRANSPORTATION OF A LARGE OBJECT BY A TEAM OF TWO ROBOTS

## ABSTRACT

In this paper dynamical systems theory is used as a theoretical language and tool to design a distributed control architecture for a team of two robots that must transport a large object and simultaneously avoid collisions with obstacles (either static or dynamic). This work extends the previous work with two robots (see [1] and [5]). However here we demonstrate that it's possible to simplify the architecture presented in [1] and [5] and reach an equally stable global behavior. The robots have no prior knowledge of the environment. The dynamics of behavior is defined over a state space of behavior variables, heading direction and path velocity. Task constrains are modeled as attractors (i.e. asymptotic stable states) of a behavioral dynamics. For each robot, these attractors are combined into a vector field that governs the behavior. By design the parameters are tuned so that the behavioral variables are always very close to the corresponding attractors. Thus the behavior of each robot is controlled by a time series of asymptotic stable states. Computer simulations support the validity of the dynamical model architecture.

## 1. INTRODUCTION

The motivation for the development of autonomous robots that are able to transport large objects arises from the potential applicability of these systems in industrials and civilian environments. There has been some research concerning this issue (e.g. [6, 7, 8, 9, 10, 12]).

One of the most and fundamental problems in controlling multiple robots carrying an object together is the maintenance of a geometric fixed configuration during the movement. This paper attempts to simplify the previous work reported in [1] and [5]. In our previous works we used the dynamical systems theory as theoretical framework to design and implement a distributed control architecture for a team of two mobile robots that had to transport a long object in cluttered environments.

As in previous work reported in [1] and [5] we assume that: (a) the robots have no prior knowledge of the environment and no path is given; (b) it is used a *leader-helper* decentralized motion control strategy, where the leader robot drives from an initial position to a final target destination (see for example [8]); (c) the helper robot ( $H_1$ ) takes the leader as a reference point and must maintain at all times a correct distance and orientation that permits to it to help the *leader* robot in the transportation task (see Figure 1).

One difference with respect to our previous work is the used support base. In the work present here, the support base gives displacements of the bar in two directions while the support base used in our previous work only gave displacements of the bar in the direction of the robot *leader* with respect to the robot  $H_1$ .

The control architecture of each robot is structured in terms of elementary behaviors. The individual behaviors and their integration are generated by non-linear dynamical system. For each behavior, desired values for the controlled behavioral variables are identified and made attractor solutions of the dynamical systems that generates the robot's motion.

The rest of the paper is structured as follows: next section presents the robot team, their tasks and the basic assumptions in this work. Next is defined and described the behavioral dynamics for the robot helper ( $H_1$ ). Results obtained from computer simulations are presented in next section. The paper ends with a brief discussion, conclusions and an outlook of future work.

## 2. ROBOT TEAM AND TASK CONSTRAINS

The simulated robots are based on the physical mobile robots used in [2], [5] and [11]. There is a difference in the support base used here with respect to the support base used in [5]. In [5] the displacement of the bar was measured only in the direction of the robot *leader* with respect to the robot *follower*. Now the support base gives displacements of the bar in two directions  $\Delta x$  and  $\Delta y$  (see Figure 2). The control and coordination are based on the main ideas presented on the previous work, but here an attempt is made to simplify the overall control architecture: (a) the behavior of each robot is controlled independently; (b) the *leader* robot knows the target position, and its task consists in moving from an initial position to a final target destination; (c) robot  $H_1$  must maintain at all times a correct orientation and distance with respect to the *leader* robot; (d) by default the  $H_1$  robot must move in an *LF/LB* formation, however if obstacles don't allow it, robot  $H_1$  must drive in *transition* or *column* formation; (e) the *leader* robot communicates to robot  $H_1$  its path velocity; (f) robot  $H_1$  is able to measure the direction at which the *leader* robot lies from its current position with respect to an external reference axis,  $\psi_{H_1, leader}$  (see

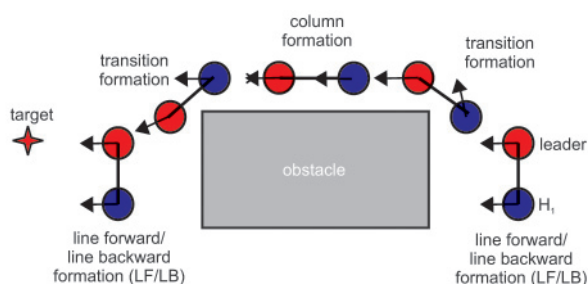
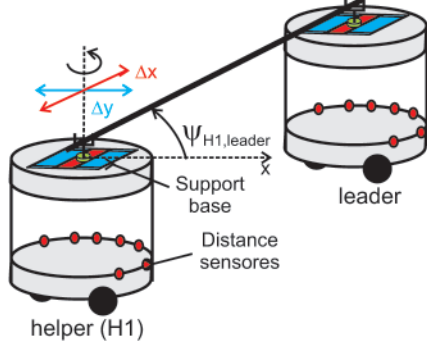


Figure 1 · Coordinated object transportation by two robots in an unknown environment. By default the robots must transport the object keeping a *line forward/line backward* formation (LF/LB). When due to encountered obstacles that is not possible robot  $H_1$  must drive in *transition* or *column* information.

Figure 2); (g) the robots don't need to know the object size, they only need to know the displacements ( $\Delta x$  and  $\Delta y$ ) of the bar in their support base (see Figure 2). (h) the robots have nonholonomic motion constrains.



**Figure 2** - Each robot has seven distance sensors mounted on a ring which is centered on the robot's rotation axis. These are used to measure the distance to obstructions at the direction in which they are pointing in space. The simulated infrared sensors have a distance range of 60 cm and an angular range of 30°. The robots are tightly coupled through a support base that permits to measure the direction at which the  $H_1$  robot sees the *leader* robot from its current position  $\psi_{H_1,leader}$  and displacements ( $\Delta x$  and  $\Delta y$ ) of the bar.

### 3. ATTRACTOR DYNAMICS FOR COORDINATED TRANSPORTATION

To model the robots behavior was used their heading direction,  $\phi$  ( $0 \leq \phi \leq 2\pi$ ), with respect to an arbitrary but fixed world axis (these external reference frame do not need to be the same for both robots), and path velocity  $\vartheta$ . Behavior is generated by continuously providing values to these variables, which control the robot's wheels. The time course of each of these variables is obtained from (constant) solutions of dynamical systems. The attractor solutions (asymptotically stable states) dominate these solutions by design.

The *leader's* heading direction and path velocity dynamics has been previously define, implemented and evaluated in [1], [5] and [11].  $H_1$ 's heading direction and path velocity dynamics are ruled by the followings dynamical systems:

$$\frac{d\phi_{H_1}(t)}{dt} = -\lambda_{H_1} \sin(\phi_{H_1} - \psi_{desired,H_1}) \quad (1)$$

$$\frac{d\vartheta_{H_1}(t)}{dt} = -c_{H_1}(\vartheta_{H_1} - V_{desired,H_1}) \left[ -\frac{(\vartheta_{H_1} - V_{desired,H_1})^2}{2\sigma_V^2} \right] \quad (2)$$

The heading direction dynamics (1) erects an attractor at  $\psi_{desired,H_1}$ , with a strength of attraction (relaxation rate) defined by  $\lambda_{H_1}$ , and a repeller in opposite direction. The path velocity dynamics (2) simple defines an attractor at the desired velocity with a relaxation rate defined by  $c_{H_1}$ . The exponential term in (2) is used to make sure that the increasing and decreasing of velocity is smooth even when the difference  $\vartheta_{H_1} - V_{desired,H_1}$  is very large.

In the next two subsections will be explain how the attractor values for heading direction and path velocity are computed from sensed and/or communicated information.

#### 3.1. Attractor dynamics for heading direction

The complete behavioral dynamics for  $H_1$  robot heading direction is governed

by (1), where  $\psi_{desired,H_1}$  is the appropriated attractor which is given by

$$\psi_{desired,H_1} = \gamma_{lf/lb} \psi_{desired,H_1,lf/lb} + \gamma_{transition} \psi_{desired,H_1,transition} + \gamma_{column} \psi_{desired,H_1,column} \quad (3)$$

where  $\psi_{desired,H_1,lf/lb}$ ,  $\psi_{desired,H_1,transition}$ ,  $\psi_{desired,H_1,column}$  are the desired directions at which the attractors are erected for each different behavior, *line forward/line backward*, *transition* and *column* formations (see Figure 3).  $\gamma_{lf/lb}$ ,  $\gamma_{transition}$  and  $\gamma_{column}$  are mutually exclusive activation variables that depending on the sensory information acquired by the distance sensors mounted on the  $H_1$  robot (see Figure 2) and the heading direction of the *leader* robot ( $\phi_{leader}(t)$ ) determine which attractor value will dominate the dynamics. In the next two subsections will be exobstacle plain how the activation variables and the attractor values are computed from sensed and/or communicated information.

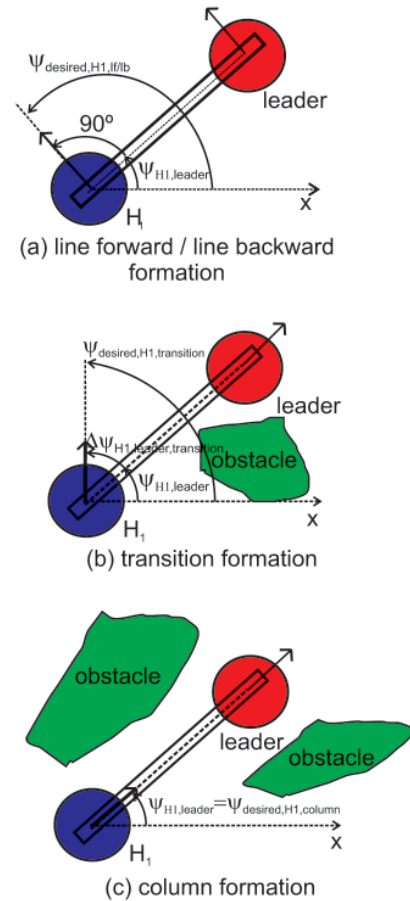


**Figure 3** - Desired orientations of  $H_1$  robot for different behaviors. In the three illustrated situations the displacement of the object is null ( $\Delta y = 0$ ). (a) *line forward/line backward* formation:  $\Delta\psi_{H_1,leader,lf/lb} = 90^\circ$ ,  $\Delta_{lf/lb,H_1,leader} = 0$  and  $k = 1$ ; (b) *transition* formation:  $\Delta\psi_{H_1,leader,transition} = 45^\circ$  and  $\Delta_{transition,H_1,leader} = 0$ ; (c) *column* formation.

#### 3.1.1. Activation variables

In the absence of obstacles, the term  $\gamma_{lf/lb}$  must dominate the dynamics, so  $\gamma_{lf/lb} = 1$ ,  $\gamma_{transition} = 0$  and  $\gamma_{column} = 0$ . This activation variable permits robot  $H_1$  to move *forward* or *backward* keeping a *line* formation with the robot *leader*. By default when no obstacles are detected, the robot  $H_1$  moves in *line forward* formation. If no obstacles are detected and the difference between the two heading directions of the robots is greater than

$\Delta\theta_1$ <sup>1</sup> and smallest that  $\Delta\theta_2$ <sup>2</sup> (correspond to the dashed line in Figure 4) the robot  $H_1$  moves in *line backward* formation. Mathematically speaking:

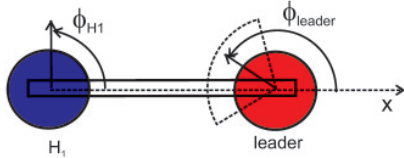


Figure 4 · When heading direction of the leader robot is pointing to the robot  $H_1$ , as illustrated here, robot  $H_1$  must move in a *line backward* formation.

$$\gamma_{lf/lb} = \begin{cases} +1, & \text{if } \alpha_{lf} = 1 \vee \alpha_{lb} = 1 \\ 0, & \text{else} \end{cases} \quad (4)$$

where  $\alpha_{lf}$  and  $\alpha_{lb}$  are the variables that signal the control architecture when it's necessary robot  $H_1$  to move forward or backward respectively.

$$\alpha_{lf} = \begin{cases} +1, & \text{if } U_{obs,H_1} \leq 0 \wedge \\ & |\phi_{H_1} - \phi_{leader}| < \Delta\theta_1 \wedge \\ & |\phi_{H_1} - \phi_{leader}| > \Delta\theta_2 \\ 0, & \text{else} \end{cases} \quad (5)$$

$$\alpha_{lb} = \begin{cases} +1, & \text{if } U_{obs,H_1} = 0 \wedge \\ & \Delta\theta_1 < |\phi_{H_1} - \phi_{leader}| < \Delta\theta_2 \\ 0, & \text{else} \end{cases} \quad (6)$$

where  $U_{obs,H_1}$  (see [1] and [5]) is the potential function of the virtual obstacles avoidance dynamics for this robot, that indicates if obstacles contributions are present. Positive values of  $U_{obs,H_1}$  indicate that  $H_1$  heading direction is in a repulsion zone of sufficient strength. Conversely, negative values of this function indicates that the heading direction is outside the repulsion range or repulsion is very weak. As showed in [1] and [5] the virtual obstacle avoidance dynamics,  $F_{obs,H_1}$  can be used to signal if obstacles are to the right or left side of the robot. Positive values of this function indicates that an obstacle is detected at the right side of the robot. Conversely, negative values of this function indicates that an obstacle is detected on the left side of  $H_1$  robot. If the value of this function is equal to zero and the potential function of the virtual obstacles avoidance dynamics ( $U_{obs,H_1}$ ) is negative, this means that none of the 7 sensors of  $H_1$  robot has detected an obstacle.  $\Delta\theta_1$  and  $\Delta\theta_2$  refers to an angular amplitude. The values used to  $\Delta\theta_1$  and  $\Delta\theta_2$  where the minimal obtained values for a safe *line backward* formation for robot  $H_1$  without losing the transported object.

When obstructions are detected and the difference between the direction  $\psi_{H_1,leader}$  and  $\phi_{leader}$  is larger than  $\Delta\theta_3$ <sup>3</sup> and the virtual obstacles avoidance dynamics ( $F_{obs,H_1}$ ) has a value different from zero, the term  $\gamma_{transition}$  must dominate the dynamics, so  $\gamma_{transition} = 1$ ,  $\gamma_{lf/lb} = 0$  and  $\gamma_{column} = 0$ . This permits robot  $H_1$  to turn around, *i.e.* avoid the obstacle by turning to the right or to the left. The  $H_1$  robot takes this decision when the following is satisfied:

<sup>1</sup>  $\Delta\theta_1$  is a fixed parameter. Here equal to 15°.

<sup>2</sup>  $\Delta\theta_2$  is a fixed parameter. Here equal to 120°.

<sup>3</sup>  $\Delta\theta_3$  is a fixed parameter. Here equal to 5°.

$$\alpha_{tr} = \begin{cases} +1, & \text{if } U_{obs,H_1} > 0 \wedge F_{obs,H_1} < 0 \\ & \wedge |\psi_{H_1,leader} - \phi_{leader}| > \Delta\theta_3 \\ 0, & \text{else} \end{cases} \quad (7)$$

$$\alpha_{tl} = \begin{cases} +1, & \text{if } U_{obs,H_1} > 0 \wedge F_{obs,H_1} > 0 \\ & \wedge |\psi_{H_1,leader} - \phi_{leader}| > \Delta\theta_3 \\ 0, & \text{else} \end{cases} \quad (8)$$

$\alpha_{tr}$  and  $\alpha_{tl}$  are variables that tells when the robot  $H_1$  has to turn to the right or to the left respectively.

$$\gamma_{transition} = \begin{cases} +1, & \text{if } \alpha_{tr} = 1 \vee \alpha_{tl} = 1 \\ 0, & \text{else} \end{cases} \quad (9)$$

Finally, if obstructions are detected and the difference between the direction  $\psi_{H_1,leader}$  and  $\phi_{leader}$  is smaller or equal to  $\Delta\theta_3$  the term  $\gamma_{column}$  must dominate the dynamics, so  $\gamma_{column} = 1$ ,  $\gamma_{lf/lb} = 0$  and  $\gamma_{transition} = 0$ . This variable is activated when

$$\gamma_{column} = \begin{cases} +1, & \text{if } U_{obs,H_1} > 0 \wedge \\ & |\psi_{H_1,leader} - \phi_{leader}| \leq \Delta\theta_3 \\ 0, & \text{else} \end{cases} \quad (10)$$

### 3.1.2. Attractor values for different behaviors

From (3) it is possible to see three desired directions ( $\psi_{desired,H_1,lf/lb}$ ,  $\psi_{desired,H_1,transition}$  and  $\psi_{desired,H_1,column}$ ), for each different behavior (see Figure 3).

#### Line forward/Line backward formation

The attractor for *Line forward* / *Line backward* formation is illustrated at top of Figure 3 and as it is possible to see its value is

$$\psi_{desired,H_1,lf/lb} = \psi_{H_1,leader} + \Delta\psi_{H_1,leader,lf/lb} + k\Delta\psi_{lf/lb,H_1,leader} \quad (11)$$

where  $\psi_{H_1,leader}$  is the direction at which robot  $H_1$  sees the robot *leader* from it's current position and  $\Delta\psi_{H_1,leader,lf/lb}$  it's an angle equal to 90° (see top of Figure 3).  $k$  is a constant that takes the value of +1 or -1 depending on the value of  $\alpha_{lf/lb}$

$$k = \begin{cases} -1, & \text{if } \alpha_{lf/lb} = 1 \\ +1, & \text{else} \end{cases} \quad (12)$$

where  $\alpha_{lf/lb}$  it is equal to +1 if robot  $H_1$  has to move in *Line backward* formation. Otherwise  $\alpha_{lf/lb}$  it is equal to 0. This is resumed in the following expression:

$$\alpha_{lf/lb} = \begin{cases} +1, & \text{if } U_{obs,H_1} = 0 \wedge \\ & \Delta\theta_1 < |\phi_{H_1} - \phi_{leader}| < \Delta\theta_2 \\ 0, & \text{else} \end{cases} \quad (13)$$

$\Delta\psi_{lf/lb,H_1,leader}$  is a sigmoidal function that varies with the displacement of the object measured by the support base of robot  $H_1$  (see Figure 5), *i.e.* it con-

verts the displacement of the object into an angle that approach null as the displacement tends to zero, and it is given by the expression

$$\Delta l_{f/lb,H_1,leader} = \frac{2 \arctan(\alpha_{H_1,leader} \Delta d)}{\pi} \quad (14)$$

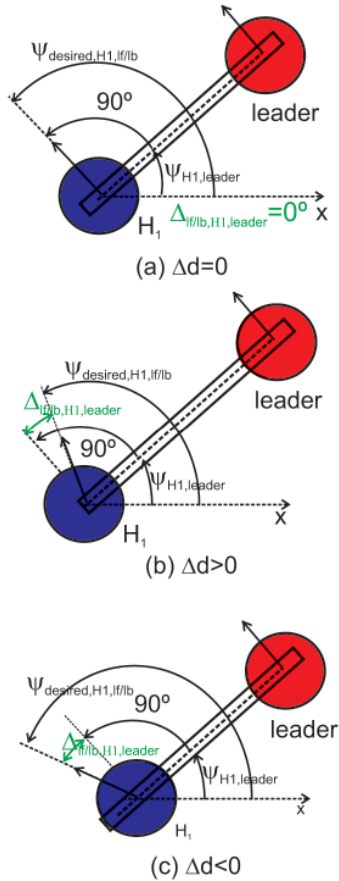


**Figure 5** - The value of  $\Delta l_{f/lb,H_1,leader}$  varies with the displacements of the object measured by the support base.

where  $\alpha_{H_1,leader}^4$  is a constant and  $\Delta d$  is the displacement of the object measured by the support base of robot  $H_1$ .

#### Transition formation

When moving around an obstacle as illustrated at the middle of Figure 3 the desired direction for robot  $H_1$  heading direction is given by:

$$\psi_{desired,H_1,transition} = \psi_{H_1,leader} + \alpha_{obs,H_1} \Delta \psi_{H_1,leader,transition} \quad (15)$$

where  $\alpha_{obs,H_1}$  is a variable that takes the value - 1 if robot  $H_1$  detects obstructions on its left side or is equal to +1 if obstructions are detected on the right side.  $\Delta \psi_{H_1,leader,transition}$  is made equal to  $45^\circ$ , this value was reached trough experimental simulations and it was the minimal necessary for a safe passage around an obstacle without colliding with it. For more details of this desired direction ( $\psi_{desired,H_1,transition}$ ) see [1] and [5].

#### Column formation

In the presence of a long obstacle or in a narrow passage, robot  $H_1$  must drive behind the *leader* robot (see bottom of Figure 3). The attractor value for  $H_1$  is directly the direction at which the *leader* robot lies as seen from the current position of the robot  $H_1$  (for more details see [1] and [5]).

$$\psi_{desired,H_1,transition} = \psi_{H_1,leader} \quad (16)$$

#### 3.2. Attractor dynamics for velocity

For the *leader's* path velocity control see [1].

The path velocity of robot  $H_1$  must be controlled so that at all times robot  $H_1$  must maintain a null displacement of the object (i.e.  $\Delta d = 0$ ). The *leader* robot communicates its current path velocity to the  $H_1$  robot. The attractor value, i.e. the required velocity  $V_{desired,H_1}$  for the velocity dynamics (2) is given by:

$$V_{desired,H_1} = \begin{cases} +v_{leader} + \frac{|\Delta d|}{v_{H_1}}, & \text{if } \Delta d < 0 \\ -v_{leader} - \frac{|\Delta d|}{v_{H_1}}, & \text{else} \end{cases} \quad (17)$$

where  $v_{H_1}$  is a constant and  $\Delta d$  is the displacement of the object measured by the support base.

#### 3.3. Hierarchy of relation rates

The finally hierarchy of relaxation rates ensures that the heading direction of  $H_1$  robot relaxes to attractor solutions as they change due to information change between the two robots.

$$\lambda_{H_1} \ll c_{H_1} \quad (18)$$

#### 4. RESULTS

The complete dynamical architecture was evaluated in computer simulations, generated by software written in MATLAB. In the simulation the robots are represented by two Cartesian coordinates and the heading direction. Cartesian coordinates are updated by a dead-reckoning rule, while the heading direction and path velocity are obtained from the corresponding behavioral dynamical. All dynamic equations are integrated with a forward Euler method with a fixed time step, and sensory information is computed once per each cycle. Distance sensors are simulated trough an algorithm reminiscent of ray tracing. The target information is defined by a goal position in space. It's assumed that the *leader* robot communicates to robot  $H_1$  its current velocity. The simulation has static and dynamic obstacles.

A simulation run in an environment with obstacles (static and dynamic), that demonstrate some features of the dynamic control architecture, is presented in Figure 6. The dynamic obstacles are represented by robots  $R3$  and  $R4$ . Their behavioral dynamics is equal to the *leader* robot and is reported in [2]. Figures 7, 8, 9 and 10 show the heading direction dynamics for robots *leader* and  $H_1$ , at the points showed in snapshots A, C, D and H.

In Figure 6 the *targets* are represented by a cross. The targets of three robots, *leader*,  $R3$  and  $R4$  are *target*, *target\_R3* and *target\_R4*, respectively. Each robot is represented by a black circle with a line that represents its heading direction.

Initially the robots are placed as illustrated in Panel A. The *leader* robot moves toward its target (Panel B) and robot  $H_1$  starts steering in a *transition* formation with the *leader* robot to avoid the obstacle at its left side. Robots

<sup>4</sup>  $\alpha_{H_1,leader}$  is a constant equal to 1.

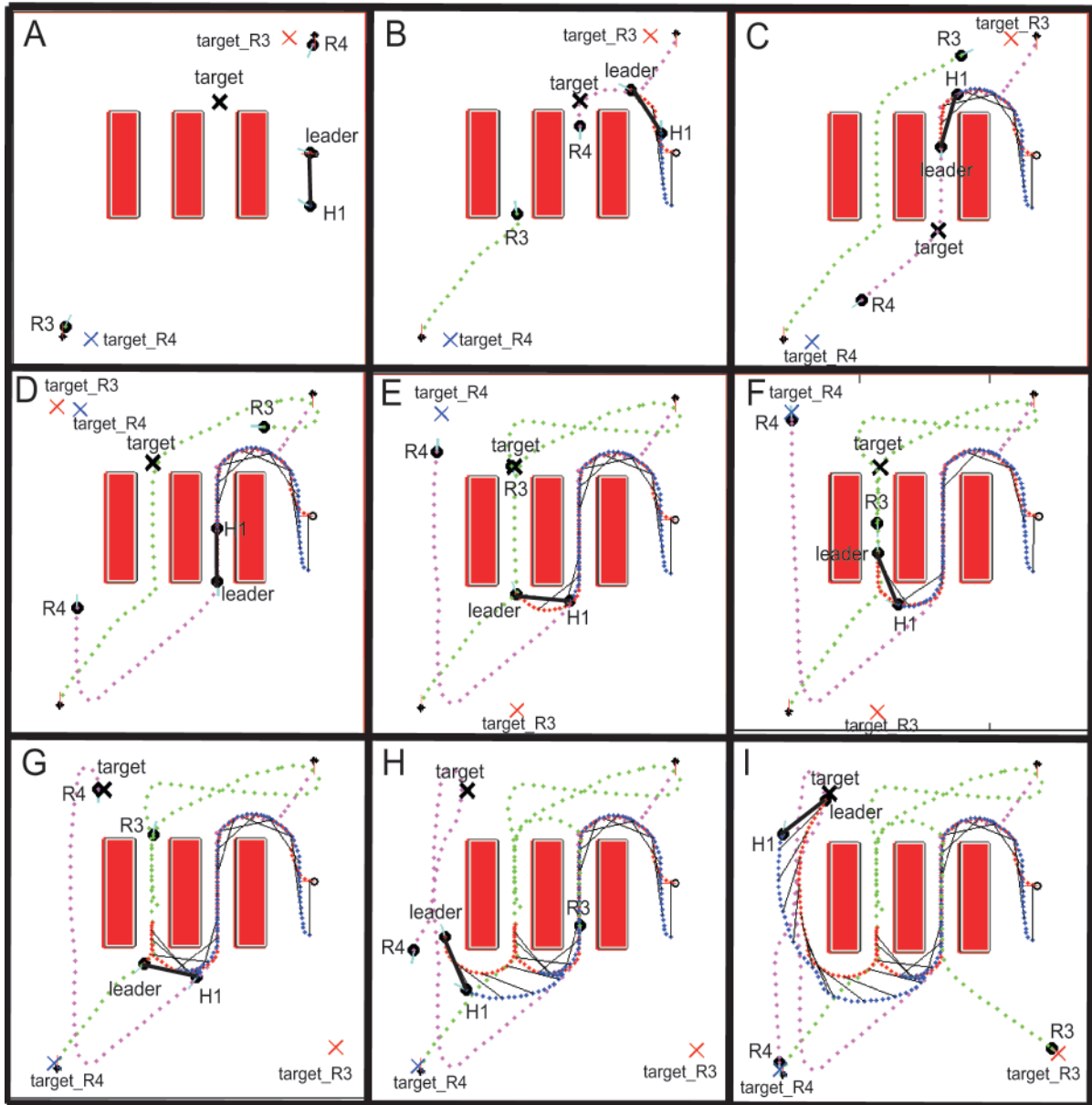


Figure 6 · Snapshots of a simulation run of the complete system.

R3 and R4 enter in different narrow passages to reach their targets. Then the *target* of leader robot is shifted to the position indicated in Panel C. This forces the leader robot to enter into the narrow passage. Robot H1 maintains a transition formation with the leader robot while entering into the narrow passage. The other two robots continue to move in direction of their targets. Then all the targets are shifted (Panel D). Robots R3 and R4 continue to move in direction of their targets. The *target\_R3* was shifted to force robot R3 to enter in the same narrow passage that the robot leader is entering. Robot H1 follows the robot leader maintaining a transition formation because it's necessary to go around the obstacle that is on its right side. Robot R4 keeps steering to its target (Panel E). Robot R3 and the leader robot stay face to face. This forces both robots to turn around and go back to get out of the narrow passage. Robot H1 drives backward (Panel F). After the leader robot gets out of the narrow passage and as soon as possible robot H1 tries to maintain a LF/LB formation with leader robot (Panel G). The leader robot must avoid the static obstacle at its right side and the dynamic obstacle (robot R4) that meanwhile appears at its left side. Robot H1 keeps

steering so as to maintain a LF/LB formation with the leader robot because it doesn't detect any obstacle (Panel H). Finally all the robots reach their targets (Panel I).

Heading directions dynamics for the two robots can be seen in Figures 7, 8, 9 and 10 at positions depicted at snapshots A, C, D and H. The black arrow in each plot indicates the current state (i.e. heading direction in the world) of the corresponding robot. As it's possible to see the heading direction of each robot is always very close to a fixed point attractor (i.e. a zero with negative slope) of the resultant dynamics (magenta line).

Panel A left plot: since no obstruction is detected by the leader robot its resulting heading direction dynamic (magenta line) is simply the target acquisition dynamic ( $f_{target,leader} = f_{leader}$ ). Panel A right plot: since no obstacles are detected by robot H1 and the difference between the two robots heading directions is smaller than  $15^\circ$  and larger than  $120^\circ$  the resultant heading direction dynamics is  $f_{H1/LB}$ . Panel C left plot: contributions of sensed

obstacles are the dashed green line ( $f_{obs,leader}$ ) and the dotted line represents the target contribution ( $f_{target,leader}$ ). The resultant dynamics (*i.e.* sum over all

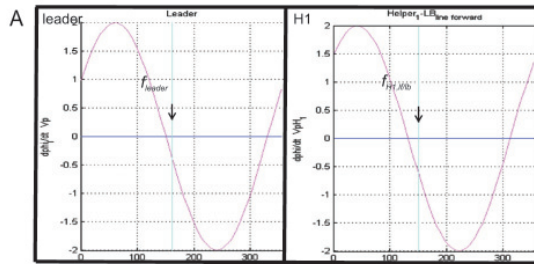


**Figure 7** · Heading direction dynamics for the two robots when they are at positions depicted in snapshot A.

contributions) is the magenta line ( $f_{leader}$ ). Panel C right plot: the  $H_1$  robot also senses obstructions (presence of  $F_{obs,H_1}$  and  $U_{obs,H_1}$ ). Because the heading direction of this robot is inside the repulsive range (positive values of  $U_{obs,H_1}$ ) and the difference the  $H_1$  robot heading direction and the direction at which the  $H_1$  robot sees *leader* robot from its current position is greater

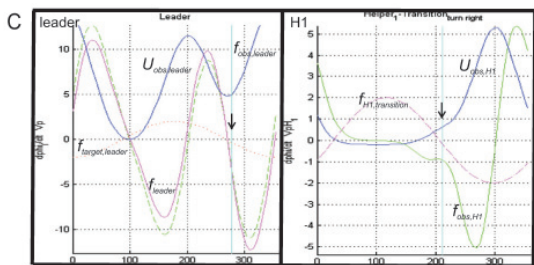


**Figure 8** · Heading direction dynamics for the two robots when they are at positions depicted in snapshot C.

than  $5^\circ$ , the resultant dynamics is governed by the term  $f_{H_1,transition}$ . Panel D left plot: it's possible to see contributions of sensed obstacles ( $f_{obs,leader}$ ) and target contribution ( $f_{target,leader}$ ). The resultant dynamics is  $f_{leader}$ . Panel D right plot: here the robot senses obstructions. Its heading direction is inside the repulsive range and the difference between the  $H_1$  robot heading

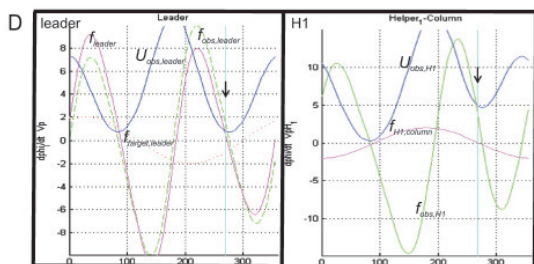


**Figure 9** · Heading direction dynamics for the two robots when they are at positions depicted in snapshot D.

direction and the direction at which the robot  $H_1$  sees *leader* robot from its current position is smaller than  $5^\circ$ , thus the resultant dynamics is dominated by the term  $f_{column,H_1}$ . Panel E left plot: the *leader* robot senses the presence of obstacle near it ( $f_{obs,leader}$ ) and so the resultant dynamics is given by the sum of obstacles contribution  $f_{obs,leader}$  and the target contribution  $f_{target,leader}$ . Panel E right plot: since no obstacles are detected by the  $H_1$  robot the resultant heading direction dynamics is  $f_{H_1,ff/br}$ .

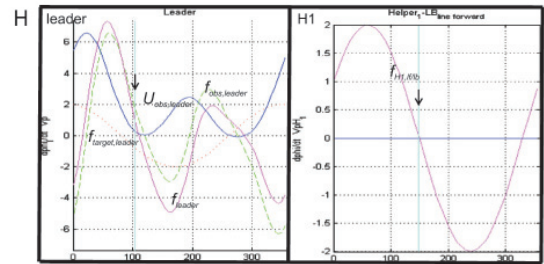


**Figure 10** · Heading direction dynamics for the two robots when they are at positions depicted in snapshot E.

## 5. CONCLUSIONS AND FUTURE WORK

We have demonstrated a very simple control architecture based on moving attractors that enables two mobile robots to carry a long object in an environment with static and dynamic obstacles. The helper has also a new feature with respect to previous work which facilitates its movement when it's needed to come backward. Most important is that the robots' behavior are stable and that the generated trajectories are smooth. The work presented here imposes of course further research. The most obvious and natural future step is the implementation of the proposed control architecture in a team of two physical robots.

## 6. ACKNOWLEDGMENTS

This work was supported, in part, through grant POSI/SRI/38051/2001 from the Portuguese Foundation and Technology (FCT), FEDER and PRODEP III. We thank Wolfram Erlhagen, Sérgio Monteiro, Luís Louro, Nzoji Hipólito, André Moreira and Toni Machado.

## REFERENCES

- [1] Soares R., Bicho E. "Using Attractor Dynamics to Generate Decentralized Motion Control of Two Robots Transporting a Long Object in Coordination". Proc. of the 2002 IEEE/RSJ Intl. Conference on Intelligent Robots and Systems, EPFL, Lausanne, 2002.
- [2] Bicho E. "Dynamic approach to Behavior-Based Robotics: design, specification, analysis, simulation and implementation". Shaker Verlag, 2000.
- [3] Schöner G. and Dose M. "A dynamical systems approach to task-level system integration used to plan and control autonomous vehicle motion". Robotics and Autonomous Systems, 10: 253-267, 1992.
- [4] Schöner G., Dose M. et al. "Dynamics of behavior: Theory and applications for autonomous robots architectures". Robotics and Autonomous Systems, 16: 213-245, 1995.
- [5] Bicho E., Louro L., et al. "Coordinated transportation with minimal explicit communication between robots". 5th IFAC Symposium on Intelligent Autonomous Vehicles (IAV), Lisbon, Portugal, July 5-7, 2004.
- [6] Ahmadabadi M. and Nakano E. "A constrain and move approach to distributed object manipulation". IEEE Transactions on Robotics and Automation, 17(2):157-172, 2001.
- [7] Chaimowicz L., Sugar T., Kumar V. and Campos V. "An architecture for tightly coupled multi-robot cooperation". in Proc. IEEE Int. Conf. Robotics and Automation, 2292-2297, 2001.
- [8] Wang Z., Takano Y., Hirata Y. and Kosuge K. "From Human to Pushing Leader Robot: Leading a Decentralized Multirobot System for Object Handling". in Proc. IEEE Int. Conf. Robotics and Biomimetics, 2004.
- [9] Ashairo Y., Chang E., Mali A. and Yamashita M. "A distributed ladder transportation algorithm for two robots in a corridor". in Proc. IEEE Int. Conf. Robotics and Automation, 3016-3021, 2001.
- [10] Hirata Y., Kume Y., Sawada T., Wang Z. and Kosuge K. "Handling of an object by multiple mobile manipulators in coordination based on caster-like dynamics". in Proc. IEEE Int. Conf. Robotics and Automation, 807-812, 2004.
- [11] Bicho E., Mallet P. and Schöner G. "Target representation on an autonomous vehicle with low level sensors". The International Journal of Robotics and Research, 19(5):424-447, 2000.
- [12] Wang Z., Takano Y., Hirata Y. and Kosuge K. "A Pushing Leader based Decentralized Control Method for Cooperative Object Transportation". in Proc. IEEE Int. Conf. Robotics and Systems, 1035-1040, 2004.